Rotationally resolved photoionization of molecular oxygen

M. Braunstein, V. McKoy, and S. N. Dixit

Citation: The Journal of Chemical Physics **96**, 5726 (1992); doi: 10.1063/1.462671
View online: http://dx.doi.org/10.1063/1.462671
View Table of Contents: http://scitation.aip.org/content/aip/journal/jcp/96/8?ver=pdfcov
Published by the AIP Publishing

Rotationally resolved photoionization of molecular oxygen

M. Braunstein[a] and V. McKoy
Arthur Amos Noyes Laboratory of Chemical Physics,[b] California Institute of Technology, Pasadena, California 91125

S. N. Dixit
Theoretical Atomic and Molecular Physics Group, Lawrence Livermore National Laboratory, L-493, Livermore, California 94550

(Received 14 August 1991; accepted 7 January 1992)

We report the results of theoretical studies of the rotationally resolved photoelectron spectra of ground state O_2 leading to the $X\,^2\Pi_g$ state of O_2^+ via the absorption of a single vacuum ultraviolet photon. These studies elaborate on a recent report [M. Braunstein *et al.*, J. Chem. Phys. **93**, 5345 (1990)] where we showed that a shape resonance near threshold creates a significant dependence of the rotational branching ratios on the ion vibrational level. We also showed that analysis of the rotational branches yields detailed information on the angular momentum composition of the shape resonance. We continue this analysis giving a comprehensive derivation of the rotationally resolved cross sections and photoelectron angular distributions. We discuss the selection rules implied by these expressions and present very high resolution cross sections ($J \rightarrow J^+$) obtained using static-exchange photoelectron orbitals and explicitly taking into account the internuclear distance dependence of the electronic transition moment. These cross sections illustrate the selection rules and show more explicitly the angular momentum composition of the shape resonance. We also present rotationally resolved photoelectron angular distributions which would be expected at low energy.

I. INTRODUCTION

Rotationally resolved photoelectron spectra of molecules can provide much insight into both the properties and dynamics of excited electronic states,[1,2] and the angular momentum composition of[3–5] and the influence of autoionization on[6–8] the electronic continuum. Recently, very high resolution threshold photoelectron spectroscopy has been used to obtain rotationally resolved photoelectron spectra of molecules.[9–12] With cooling in a supersonic nozzle, rotationally resolved spectra were obtained for photoionization of the ground state of O_2 ($X\,^3\Sigma_g^-$) leading to the ground state ($X\,^2\Pi_g$) of O_2^+ via a single vacuum ultraviolet (VUV) photon.[13] The spectral transitions of interest here are illustrated schematically in Fig. 1. Figure 2 shows the measured rotational spectra for vibrational levels $v^+ = 0$, 1, and 2 of the ion along with the results of our calculations as given in Ref. 13 (note that the ground state spin splitting is not resolved). Analysis of the calculated transition amplitudes showed that these rotational branches were dominated by specific components of the angular momentum of the photoelectron, with the lower ΔN peaks ($\Delta N = N^+ - N$) arising primarily from $l = 1$ and the higher ΔN from $l = 3$. Furthermore, with increasing vibrational excitation of the ion, the $l = 1$ partial wave increases in importance and leads to a dependence of the rotational branching ratios on the ion vibrational level. This dependence of the photoelectron angular momentum composition on vibrational level arises from a shape resonance near threshold which has been previously observed and studied in vibrationally resolved spectra.[14–24] In the absence of a shape resonance, which induces this dependence of the electronic transition moment on the internuclear distance, the same ratio of $l = 1$ to $l = 3$ amplitudes is expected within each vibrational level and there should be no such vibrational state dependence of the rotational branching ratios.

In this paper, we present a comprehensive derivation of the formulation we use in our studies of the rotationally resolved cross sections and photoelectron angular distributions for these transitions, including a full description of the mixed Hund's case (a)–(b) ionic ground state. We discuss the selection rules implied by these expressions and present very high resolution (with the ground state spin splitting resolved) cross sections, obtained with Hartree–Fock photoelectron orbitals, which more plainly reveal the angular momentum composition of the shape resonance. We also present calculated photoelectron angular distributions expected at low photoelectron energy. The difference in the angular momentum composition for low ΔN peaks vs high ΔN is especially evident in these photoelectron angular distributions.

II. THEORY

We extend the formulation given previously[25] to treat transitions from a Hund's case (b) resonant state to a mixed Hund's case (a)–(b) ion which is especially appropriate for the $^3\Sigma \rightarrow {}^2\Pi$ transition[26] of interest in the photoionization of O_2. The development closely follows the work of Buck-

[a] Present address: T-12 Division, Mail Stop B-268, Los Alamos National Laboratory, Los Alamos, New Mexico 87545.
[b] Contribution No. 8489.

0021-9606/92/085726-08$06.00

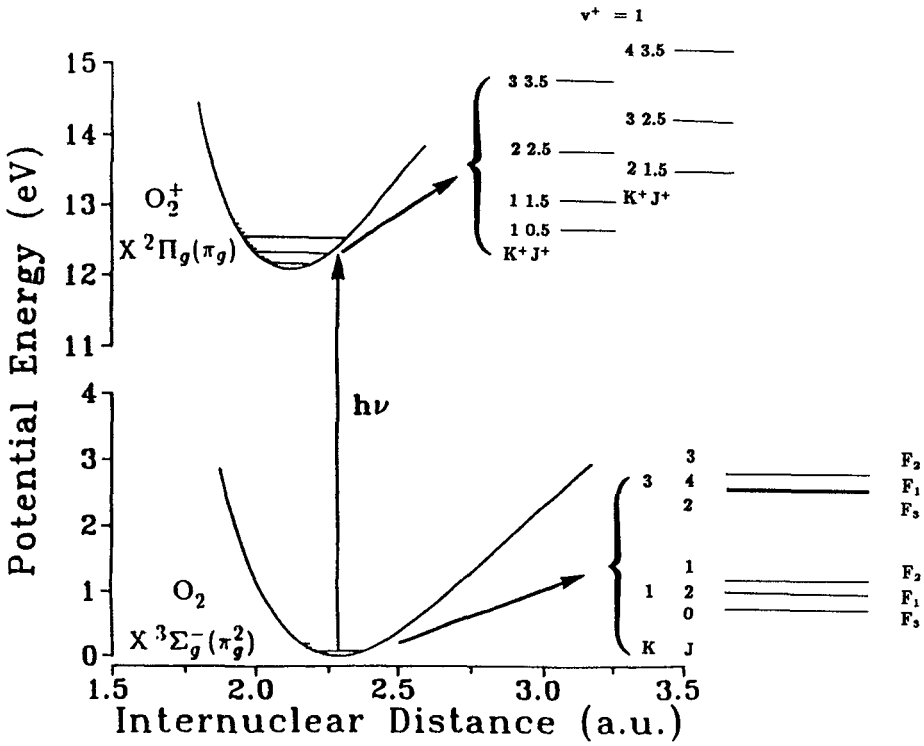

FIG. 1. Diagram illustrating the rotationally resolved photoelectron spectra for photoionization of O_2 ($X\,^3\Sigma_g^-$) by a single VUV photon. The left side of the figure shows the potential curves of the ground and ion states, while the right side shows some of the rotational states of an ion vibrational level and the first few rotational states of the ground vibrational level of the $X^2\Sigma_g^-$ electronic ground state.

ingham *et al.*,[27] but includes the effects of mixing of the Hund's cases (a) and (b) in the final ionic state.

The differential cross section for photoionization of a rotational state J leading to an ion in an angular momentum state J^+ is given by

$$\sigma_{J\to J^+}(\theta,\phi) = \frac{4\pi^2 E}{c} P_{m_J} \times \sum_{m_J m_J^+ m_s(c,d)} |\langle \Psi_f^{J^+} | D_{\mu_0} | \Psi_i^J \rangle|^2, \tag{1}$$

where E is the photon energy, c is the speed of light, m_J is the projection of J on the laboratory z axis, m_J^+ is the projection of J^+ on the laboratory z axis, and m_s is the projection of the photoelectron spin on the laboratory z axis. The notation (c,d) implies a sum over the c and d parity states of the ion.[28] P_{m_J} is the statistical weight of the initial m_J states, which for an isotropic distribution is given by $e^{-E_J/kT}/Z$, where $Z = \Sigma_{J'}(2J'+1)e^{-E'_J/kT}$. In Eq. (1), $\Psi_f^{J^+}$ is the final state

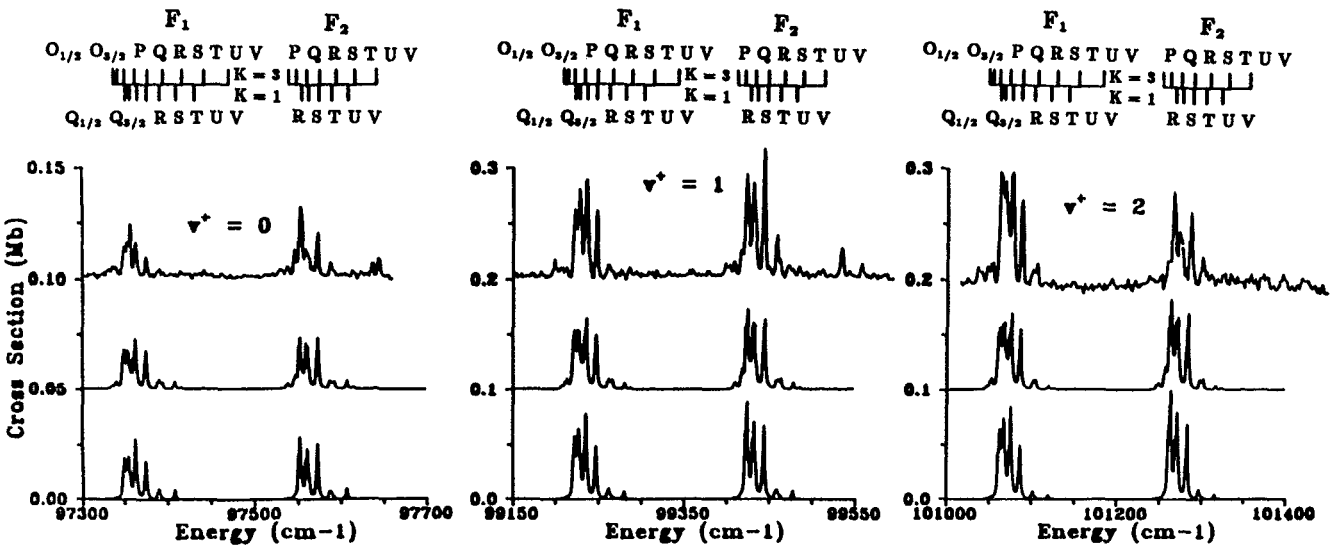

FIG. 2. Threshold rotationally resolved photoelectron spectra for single-photon ionization of O_2 ($X\,^3\Sigma_g^-$) leading to $v^+ = 0$, 1, and 2 levels of O_2^+ ($X\,^2\Pi_g$): measured spectra at about 10 K (top frame); calculated spectra at 10 K (center frame); calculated spectra at 5 K (bottom frame). These spectra are taken from Ref. 13. The branch designations refer to $\Delta N = (N^+ - N)$ transitions. For example, an S branch under F_1 on the bottom row of letters refers to a transition from the $N = 1$ rotational level of the ground state to the $N^+ = 3$ level of the F_1 spin–orbit manifold of the ion. (We have switched to the more modern notation for the total angular momentum excluding spin, replacing K of Ref. 13 with N.) The calculated spectra have an assumed linewidth of 2 cm^{-1}. The experimental spectra have arbitrary intensity units. The base lines of the 10° spectra have been shifted upward by a constant amount.

wave function (ion plus photoelectron), Ψ_i^J is the initial target state, and D_{μ_0} is the dipole moment operator where μ_0 characterizes the polarization of the radiation. For the initial state case (b) wave function, we use the Born–Oppenheimer approximation so that[28]

$$|\Psi_i^J\rangle = |\gamma v \Lambda N S J M_J\rangle$$

$$= \sum_{MM_s} \langle NMSM_S|JM_J\rangle |SM_S\rangle \psi^e_{\gamma\Lambda}(\{r_i'\};R)\chi_v(R) \times (-1)^{M-\Lambda} D^N_{M\Lambda}(\hat{R}) \sqrt{\frac{2N+1}{8\pi^2}}, \quad (2)$$

where $\psi^e_{\gamma\Lambda}(\{r_i'\};R)$ is the electronic wave function, χ_v is the wave function for the vibrational state v, and $D^N_{M\Lambda}(\hat{R})$ is a symmetric top rotational wave function with total angular momentum (excluding spin) of N. M and Λ are the projections of N along the laboratory z axis and the molecular z axis ($\Lambda = 0$ for Σ states, $\Lambda = \pm 1$ for Π states), respectively, J is the total angular momentum including spin, ($\mathbf{J} = \mathbf{N} + \mathbf{S}$), and M_J its projection along the laboratory z axis. S is the total spin with a projection M_S on the laboratory z axis, and γ contains all other subscripts needed for an unambiguous designation of the state. Due to the many-particle nature of the wave function, and for reasons which will be made clear later, it is convenient to transform the spin in Eq. (2) into the molecular frame. We then have[29]

$$|\gamma v \Lambda N S J M_J\rangle$$

$$= \sum_{M,M_s,\Sigma} \langle NMSM_S|JM_J\rangle |S\Sigma\rangle \psi_{\gamma'\Lambda}(\{r_i'\};R)\chi_v(R) \times (-1)^{M-\Lambda} D^N_{M\Lambda}(\hat{R})(-1)^{\Sigma - M_s} \times D^S_{M_s\Sigma}(\hat{R}) \sqrt{\frac{2N+1}{8\pi^2}}, \quad (3)$$

where Σ is the projection of S on the molecular z axis.

It is well known that the rotational states of the $X\,^2\Pi_g$ ion of O_2 do not belong to a pure Hund's case coupling. In the low J^+ limit, they can be best described by Hund's case (a), while for high J^+ the rotational levels are best described using Hund's case (b).[26] Since we wish to describe a wide range of J^+ here, we use a mixed rotational basis. This is done by expanding the rotational wave function in Hund's case (a) basis functions with $\Omega^+ = 1/2$ and $\Omega^+ = 3/2$ and diagonalizing the rotational Hamiltonian, as discussed by Hougen.[30] The energy levels and rotational wave functions with this mixed basis are given in Appendix A. The wave function for the final state can therefore be written as

$$|\Psi_f^{J^+}\rangle = \Big[\frac{c_1(J^+)}{\sqrt{2}}(|\gamma^+\Lambda^+S^+\Sigma^+\Omega^+_{1/2}J^+M_J^+\rangle \pm |\gamma^+ - \Lambda^+S^+ - \Sigma^+ - \Omega^+_{1/2}J^+M_J^+\rangle) + \frac{c_2(J^+)}{\sqrt{2}}(|\gamma^+\Lambda^+S^+\Sigma^+\Omega^+_{3/2}J^+M_J^+\rangle \pm |\gamma^+ - \Lambda^+S^+ - \Sigma^+ - \Omega^+_{3/2}J^+M_J^+\rangle)\Big]|\phi_k\rangle, \quad (4)$$

where c_1 and c_2 are coefficients which depend on J^+ and are given in Appendix A, the $+$ and $-$ combinations describe c and d parity states of the ion, respectively, and $\Omega^+ = \overline{\Lambda}^+ + \Sigma^+$ and $\overline{\Lambda}^+ = |\Lambda^+|$ (see Ref. 28). Here $|\phi_k\rangle$ is the photoelectron wave function. The final-state wave function therefore consists of linear combinations of four "primitive" wave functions of the form,

$$|\gamma^+ v^+ \Lambda^+ S^+ \Sigma^+ \Omega^+ J^+ M_J^+\rangle|\phi_k\rangle = \sqrt{\frac{2J^+ + 1}{8\pi^2}}\psi^e_{\gamma^+\Lambda^+}(\{r_i\};R)|S^+\Sigma^+\rangle \times \chi_v^+(R)(-1)^{M_J^+ - \Omega^+} D^{J^+}_{M_J^+\Omega^+}(\hat{R})|\phi_k\rangle. \quad (5)$$

The photoelectron wave function $|\phi_k\rangle$ can be expanded in partial waves,

$$|\phi_k\rangle = \sum_{lm\lambda} \psi_{kl\lambda}(r';R) i^l e^{-i\eta_l}(-1)^{m-\lambda} Y^*_{lm}(\hat{k}) D^l_{m\lambda} \times (\hat{R})|\tfrac{1}{2}m_s\rangle, \quad (6)$$

where k denotes the momentum of the photoelectron and $\hat{k}$ its direction in the laboratory frame. $lm\lambda$ denote the angular momentum of the photoelectron and its projections along the laboratory and molecular frame z axes, respectively, $\frac{1}{2}$ is the electron spin and m_s its projection on the laboratory z axis. Again it is convenient to transform the spin into the molecular frame so that we have

$$|\phi_k\rangle = \sum_{lm\lambda m_\sigma} \psi_{kl\lambda}(r';R) i^l e^{-i\eta_l}(-1)^{m-\lambda} Y^*_{lm}(\hat{k}) \times D^l_{m\lambda}(\hat{R})(-1)^{m_\sigma - m_s} D^{1/2}_{m_s m_\sigma}|\tfrac{1}{2}m_\sigma\rangle, \quad (7)$$

where m_σ is the projection of the electron spin on the molecular z axis. The dipole moment operator for polarized light can be written

$$D_{\mu_0} = (4\pi/3)^{1/2} \sum_s r_s Y_{1\mu_0}(\hat{r}_s), \quad (8)$$

where μ_0 characterizes the polarization of the light; $\mu_0 = 0$ for light linearly polarized along the laboratory z axis, $\mu_0 = \pm 1$ for circularly polarized light propagating along the laboratory z axis. It is necessary to transform the dipole moment operator into the molecular frame so that

$$D_{\mu_0} = (4\pi/3)^{1/2} \sum_s r_s \sum_\mu (-1)^{\mu-\mu_0} D^1_{\mu_0\mu} Y_{1\mu}(\hat{r}'_s). \quad (9)$$

Using Eqs. (1) and (4), we have

$$\sigma_{J^+ \leftarrow J}(\theta,\phi) = \frac{4\pi^2 E}{c} P_{m_J} \sum_{m_J m_J^+ m_s(c,d)} \Big| \frac{c_1}{\sqrt{2}}[M_{fi}(\Omega^+_{1/2}) \pm M_{fi}(\Omega^+_{-1/2})] + \frac{c_2}{\sqrt{2}}[M_{fi}(\Omega^+_{3/2}) \pm M_{fi}(\Omega^+_{-3/2})]\Big|^2, \quad (10)$$

where the "primitive" matrix elements are given by

$$M_{fi} = \langle \gamma^+ v^+ \Lambda^+ S^+ \Sigma^+ \Omega^+ J^+ M_{J^+}; \phi_k | D_{\mu_0} | \gamma v \Lambda K S J M_J\rangle. \quad (11)$$

Using Eqs. (3), (5), (7), and (9) these primitive matrix elements can be written as[29]

$$M_{fi} = \sqrt{\frac{4\pi}{3}} \sum_{lm\lambda\mu\Sigma m_\sigma \Omega J_t M_t \Omega_j m_j \Omega_j} (2j+1)(2J_t+1)\sqrt{(2J^++1)(2N+1)(2J+1)(2S+1)}$$
$$\times(-1)^{M_{J^+}-\Omega^++m-\lambda+\Omega-N+S-\Sigma}(-i)^l e^{i\eta_l} Y_{lm}(\hat{k}) I_{fi}^{\text{avg}}(\Lambda^+\Sigma^+ l\lambda\mu m_\sigma)$$
$$\times\begin{pmatrix} S^+ & 1/2 & S \\ \Sigma^+ & m_\sigma & -\Sigma \end{pmatrix}\begin{pmatrix} N & S & J \\ \Lambda & \Sigma & -\Omega \end{pmatrix}\begin{pmatrix} J^+ & J & J_t \\ -M_{J^+} & M_J & M_t \end{pmatrix}\begin{pmatrix} J^+ & J & J_t \\ -\Omega^+ & \Omega & \Omega_t \end{pmatrix}$$
$$\times\begin{pmatrix} J_t & j & 1/2 \\ -M_t & -m_j & -m_s \end{pmatrix}\begin{pmatrix} J_t & j & 1/2 \\ -\Omega_t & -\Omega_j & -m_\sigma \end{pmatrix}\begin{pmatrix} l & 1 & j \\ -\lambda & \mu & \Omega_j \end{pmatrix}\begin{pmatrix} l & 1 & j \\ -m & \mu_0 & m_j \end{pmatrix}, \tag{12}$$

where J_t denotes the angular momentum transferred to the ion, and M_t and Ω_t denote the projection of J_t along the laboratory and molecular z axes, respectively. The indices j, m_j, and λ_j are dummy indices. Here the vibrationally resolved amplitudes are

$$I_{fi}^{\text{avg}}(\Lambda^+\Sigma^+ l\lambda\mu m_\sigma) = \int dR \chi_{v^+}^*(R)\chi_{v_i}(R) I_{fi} \times(R;\Lambda^+\Sigma^+ l\lambda\mu m_\sigma) \tag{13}$$

and

$$I_{fi}(R;\Lambda^+\Sigma^+ l\lambda\mu m_\sigma) = \sum_{\text{composite final states}} \langle\psi^e_{\gamma\Lambda^+}|\langle S^+\Sigma^+|\langle\psi_{kl\lambda}| \times\langle\tfrac{1}{2}m_\sigma|\psi_f^{\text{composite}}\rangle, \tag{14a}$$

$$\langle\psi_f^{\text{composite}}|rY_{1\mu}|A\psi_\gamma\Lambda^e\rangle|S\Sigma\rangle = O_{fi}\bar{I}_{fi}, \tag{14b}$$

where these wave functions are antisymmetrized and $\psi_f^{\text{composite}}$ are the composite final states as given in Appendix B. The re-expansion of the composite $\bar{I}_{fi}$ amplitudes in terms of I_{fi} amplitudes therefore comes from the necessity of defining final state basis functions for the molecular ion which have a well-defined Λ^+ projection. This occurs in Σ_u^- composite states ($k\pi_u$ photoelectron), where the composite final state wave function is built on a linear combination of Λ^+ and $-\Lambda^+$ ion cores. The overlaps O_{fi} are simply constants. The composite amplitudes $\bar{I}_{fi}$ have been evaluated previously in the context of vibrationally resolved transitions.[14] Details are given elsewhere.[14,31,32] It is important to note, however, that these amplitudes are obtained in the static-exchange approximation and in the fully anisotropic potential of the molecular ion and include the effects of the internuclear dependence of the electronic transition amplitude via Eq. (13). We have now completely defined the quantities needed to obtain the rotationally resolved differential cross section.

An alternative way of expressing the differential cross section, which is sometimes more convenient, is in terms of expansion coefficients B_{LM},

$$\sigma_{J^+\_\_J}(\theta,\phi) = \sum_{m_J m_{J^+} m_s(c,d)} \sum_{LM} B_{LM} Y_{LM}(\theta,\phi), \tag{15}$$

where

$$B_{LM} = \frac{4\pi^2 E}{c} P_{m_J} \sum_{ll'mm'} \langle\Psi_f^{J^+}|D_{\mu_0}|\Psi_i^J\rangle\langle\Psi_f^{J^+}|D_{\mu_0}|\Psi_i^J\rangle^* \times\left[\frac{(2l+1)(2l'+1)(2L+1)}{4\pi}\right]^{1/2} \times\begin{pmatrix} l & l' & L \\ m & -m' & -M \end{pmatrix}\begin{pmatrix} l & l' & L \\ 0 & 0 & 0 \end{pmatrix} \times(-1)^{m'-M}, \tag{16}$$

where we have taken out the sum over l, l', m, and m' in the matrix element and shown it explicitly. The angle-integrated cross section is

$$\sigma_{\text{tot}} = \sqrt{4\pi} B_{00}, \tag{17}$$

and

$$\beta = \frac{B_{20}}{B_{00}}\sqrt{5}, \tag{18}$$

where β is the familiar asymmetry parameter,[33]

$$\sigma(\theta,\phi) = \frac{\sigma_{\text{tot}}}{4\pi}[1+\beta P_2(\cos\theta)], \tag{19}$$

and $P_2(\cos\theta)$ is a Legendre polynomial. A computationally convenient expression for the angle-integrated cross section can be obtained by separating the laboratory and molecular frame projection indices and summing over the laboratory frame m projections. From Eq. (1) we have

$$\sigma_{\text{tot}} = \frac{4\pi^2 E}{c} P_{m_J} \sum_{m_J m_J^+ m_\sigma(c,d)} \int |\langle\Psi_f^{J^+}|D_{\mu_0}|\Psi_i^J\rangle|^2 d\Omega(\hat{k}). \tag{20}$$

Expanding in terms of the "primitive" matrix elements we obtain,

$$\sigma_{\text{tot}} = \frac{4\pi^2 E}{c} P_{m_J} \times \sum_{m_J m_J^+ m_\sigma(c,d)} \int \left| \frac{c_1}{\sqrt{2}}[M_{fi}(\Omega^+_{1/2}) \pm M_{fi}(\Omega^+_{-1/2})] + \frac{c_2}{\sqrt{2}}[M_{fi}(\Omega^+_{3/2}) \pm M_{fi}(\Omega^+_{-3/2})] \right|^2 d\Omega(\hat{k}). \tag{21}$$

The primitive amplitudes can be separated into a laboratory frame part and molecular frame contributions so that

$$\sigma_{\rm tot} = \frac{4\pi^2 E}{c} P_{m_J} \sum_{m_J, m_j^+, m_s(c,d)} \int M_{fi}^{\rm lab}(M_{fi}^{\rm lab})^* d\Omega_{\hat{k}} \times \left| \frac{c_1}{\sqrt{2}} [M_{fi}^{\rm molecule}(\Omega_{1/2}^+) \pm M_{fi}^{\rm molecule}(\Omega_{-1/2}^+)] + \frac{c_2}{\sqrt{2}} [M_{fi}^{\rm molecule}(\Omega_{3/2}^+) \pm M_{fi}^{\rm molecule}(\Omega_{-3/2}^+)] \right|^2, \quad (22)$$

where

$$M_{fi}^{\rm lab} = \sqrt{\frac{4\pi}{3}} \sqrt{(2N+1)(2J+1)}(-1)^{m_J+\mu_0-m_s} \sum_{lmJ_t jM_t m_j} (2j+1)(2J_t+1) \times \begin{pmatrix} J^+ & J & J_t \\ -M_J^+ & M_J & M_t \end{pmatrix} \begin{pmatrix} J_t & j & \frac{1}{2} \\ -M_t & -m_j & -m_s \end{pmatrix} \begin{pmatrix} l & 1 & j \\ -m & \mu_0 & m_j \end{pmatrix} (-i)^l e^{i\eta_l} Y_{lm}^*(\hat{k}), \quad (23)$$

and

$$M_{fi}^{\rm molecule} = \sum_{\lambda\mu\Sigma m_\sigma \Omega\Omega_t \lambda_j} (-1)^{-\Omega^+ - \lambda + \Omega - N + S - \Sigma} \sqrt{(2J+1)(2S+1)} \begin{pmatrix} S^+ & \frac{1}{2} & S \\ \Sigma^+ & m_\sigma & -\Sigma \end{pmatrix} \begin{pmatrix} N & S & J \\ \Lambda & \Sigma & -\Omega \end{pmatrix} \times \begin{pmatrix} J^+ & J & J_t \\ -\Omega^+ & \Omega & \Omega_t \end{pmatrix} \begin{pmatrix} J_t & j & \frac{1}{2} \\ -\Omega_t & -\lambda_j & -m_\sigma \end{pmatrix} \begin{pmatrix} l & 1 & j \\ -\lambda & \mu & \lambda_j \end{pmatrix} I_{fi}^{\rm avg}. \quad (24)$$

Integration over $\Omega_{\hat{k}}$ and summation over m_J, m_j^+, and m_s, lead to the compact expression,

$$\sigma_{\rm tot} = \frac{4\pi^2 E}{c} P_{m_J} \frac{4\pi}{9} (2N+1)(2J_+ + 1) \times \sum_{jJ_t lm(c,d)} (2j+1)(2J_t+1) \times \left| \frac{c_1}{\sqrt{2}} [M_{fi}^{\rm molecule}(\Omega_{1/2}^+) \pm M_{fi}^{\rm molecule}(\Omega_{-1/2}^+)] + \frac{c_2}{\sqrt{2}} [M_{fi}^{\rm molecule}(\Omega_{3/2}^+) \pm M_{fi}^{\rm molecule}(\Omega_{-3/2}^+)] \right|^2. \quad (25)$$

This expression for the total cross section is considerably more efficient computationally than Eq. (17).

III. HIGH RESOLUTION RESULTS: SELECTION RULES

In Fig. 3, we show our calculated high-resolution threshold spectrum for photoionization of the ground state of O_2 leading to the $v^+ = 2$ level of O_2^+ ($^2\Pi_g$) at a rotational temperature of 5 K and for the F1 spin–orbit manifold. The peaks have an assumed bandwidth of 0.25 cm^{-1}. These peaks may, however, still be evident at a lower resolution. The peaks seen in Fig. 2 are now split into three components so that the individual J levels of the ground state are resolved. We can now see the spin splitting of the ground state and have a fully resolved $J \rightarrow J^+$ transition.

From Eqs. (24) and (25) the transition amplitude can be seen to depend on the product of $3-j$ symbols,

$$\begin{pmatrix} J^+ & J & J_t \\ -\Omega^+ & \Omega & \Omega_t \end{pmatrix} \begin{pmatrix} J_t & j & \frac{1}{2} \\ -\Omega_t & -\lambda_j & -m_\sigma \end{pmatrix} \times \begin{pmatrix} l & 1 & j \\ -\lambda & \mu & \lambda_j \end{pmatrix}.$$

For certain $J \rightarrow J^+$ transitions, this dependence restricts the allowed partial waves of the photoelectron *to a single component*. For example, for the transition $J = 0 \rightarrow J^+ = 0.5$ (Q branch), only the $l = 1$ partial wave is allowed. The transitions $J = 0 \rightarrow J^+ = 3.5$ (S branch), $J = 0 \rightarrow J^+ = 4.5$ (T branch), and all the U branch transitions, do not allow the $l = 1$ wave. Being so close to threshold, the intensity due to these higher partial waves (really only $l = 3$ since $l = 5$ and higher are negligible) signal the presence of a shape resonance near threshold. Such "fully resolved" transitions are dynamically significant because they decompose the continuum into single partial waves and offer a "snapshot" of the photoelectron continuum. Furthermore, if we now monitor these same rotational transitions for different vibrational

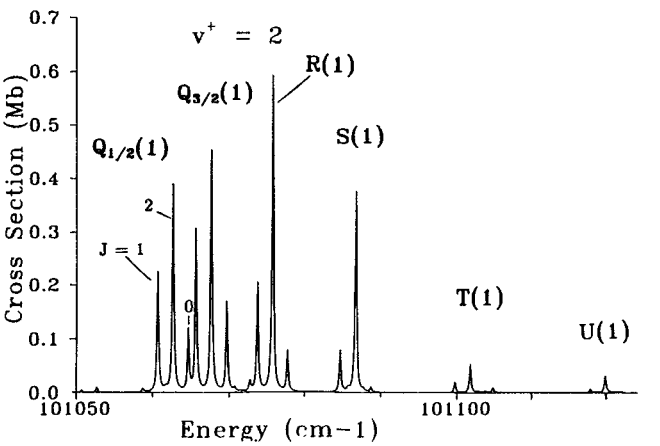

FIG. 3. The same as Fig. 2, except here we focus on the calculated F1 component of the $v^+ = 2$ vibrational level at 5 K. We have assumed a linewidth of 0.25 cm^{-1} so that the ground state spin splitting is now visible.

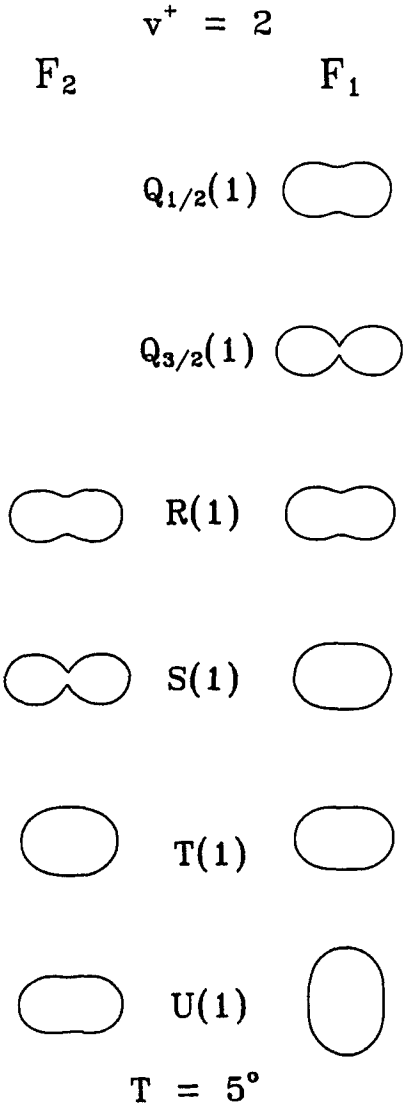

FIG. 4. Calculated rotationally resolved photoelectron angular angular distributions leading to the $v^+ = 2$ level of O_2^+ at 5 K.

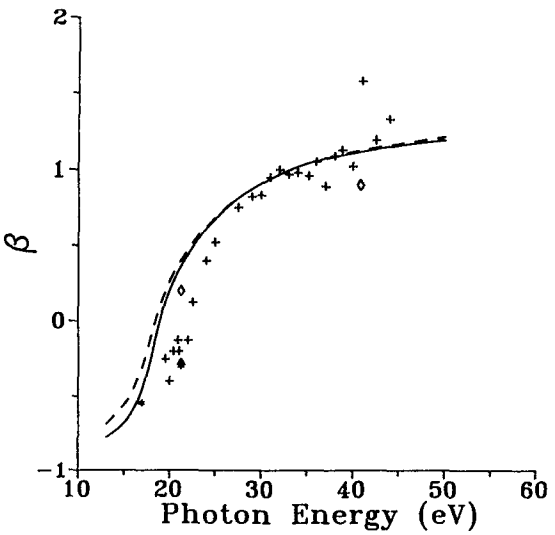

FIG. 5. Vibrationally and rotationally unresolved photoelectron asymmetry parameters for photoionization of the ground state of O_2 leading to O_2^+ ($^2\Pi_g$). —, present results (length form of the photoelectron matrix element); – – –, present results (velocity); +, experimental data of Ref. 37; *, experimental data of Ref. 38; △, experimental data of Ref. 39; ◇, experimental data of Ref. 40.

levels, we can see the changing partial wave character of the continuum brought about by the internuclear distance dependence of the electronic transition moment induced by the shape resonance. These selection rules may also be important in understanding Hund's case (b) to mixed case (a) transitions in other molecules.[34] Experiments are now underway[35] on single-photon VUV ionization of ground state HCl to the ground state $X\,^2\Pi$ ion. Here the absence of gerade–ungerade symmetry may make the selection rules weaker since most transitions will now be mixtures of even and odd partial waves.

IV. PHOTOELECTRON ANGULAR DISTRIBUTIONS

In Fig. 4 we show our calculated photoelectron angular distributions for near-threshold energies (50 meV) for $v^+ = 2$. The angular distributions for the other vibrational levels are similar and are not shown. In this figure, the light is propagating into the page and the direction of polarization is vertical. For ease of viewing, each transition is normalized to have the same integrated intensity. For low ΔN transitions, most of the photoelectron flux is ejected perpendicular to the plane of polarization, giving a value of β close to -1. For higher ΔN transitions, the distribution appears more isotropic with a β close to zero. These angular distributions dramatically show that there is a change in the partial wave character of the continuum with rotational branch, and mirror the dominance of the $l = 1$ waves for low ΔN and the $l = 3$ waves for high ΔN. Such dependence of photoelectron angular distributions on the final rotational state has been observed before in resonance enhanced multiphoton ionization studies,[36] but to our knowledge not in ground state photoionization.

For completeness, our calculated rotationally and vibrationally *unresolved* photoelectron asymmetry parameter β along with the measured values[37–40] are shown in Fig. 5. Near threshold, β is close to -1, rises steeply with increasing photon energy, and reaches a plateau near $+1$ at high energy. The value of near -1 close to threshold is consistent with the rotationally resolved results, if we note that the low ΔN levels are indeed the most intense in each rotational band.

ACKNOWLEDGMENTS

Research at the California Institute of Technology was supported by grants from the National Science Foundation (Grant No. CHE-85121391), AFOSR (Grant No. 87-0039), and the Office of Health and Environmental Research of the DOE (Grant No. DEFG03-87ER60513). We also acknowledge use of the resources of the San Diego Supercomputer Center, which is supported by the National Science Foundation. Work done by S. N. D. was performed under the auspices of the U.S. Department of Energy by

Lawrence Livermore National Laboratory under Contract No. W-7405-Eng-48.

APPENDIX A

Following Hougen,[30] we derive rotational wave functions for the mixed Hund's (a)–(b) from a basis of pure Hund's case (a) for a $^2\Pi$ ion. We write the total Hamiltonian as

$$H = H_{ev} + H_r, \tag{A1}$$

where

$$H_{ev} = \text{electronic} - \text{vib} + AL_zS_z, \tag{A2}$$

and

$$\begin{aligned} H_r &= \text{rotational} \\ &= B(R_x^2 + R_y^2) \\ &= B\left[(J^2 - J_x^2 + L^2 - L_z^2 + S^2 - S_z^2)\right. \\ &\quad + (S_+L_- + S_-L_+) \\ &\quad - (J_+S_- + J_-S_+) \\ &\quad \left. - (J_+L_- + J_-L_+)\right]. \end{aligned} \tag{A3}$$

Here A is the spin–orbit constant and B is the rotational constant. For an isolated $^2\Pi$ state, we have,

$$\begin{aligned} H &= e - v + AL_zS_z + B\left[(J^2 - J_z^2 + S^2 - S_z^2 + L_{1^2}\right. \\ &\quad \left. - (J_+S_- + S_-J_+)\right]. \end{aligned} \tag{A4}$$

Using the pure Hund's case (a) basis, $|\Lambda S\Sigma;\Omega JM\rangle$, we have for the Hamiltonian matrix, $\langle H\rangle$,

$$\begin{Bmatrix} -\frac{1}{2}A + B(J+1/2)^2 & -B\left[(J+\frac{1}{2})^2 - 1\right]^{1/2} \\ -B\left[(J+\frac{1}{2})^2 - 1\right]^{1/2} & \frac{1}{2}A + B\left[(J+\frac{1}{2})^2 - 2\right] \end{Bmatrix}. \tag{A5}$$

This leads to a secular equation for the rotational energy with roots

$$E_\pm = B\left[(J+1/2)^2 - 1\right] \pm 1/2BX, \tag{A6}$$

where

$$X = \left[(J+1/2)^2 + \lambda(\lambda-4)\right]^{1/2}, \tag{A7}$$

and $\lambda = A/B$. These energies correspond to the F1 and F2 components, respectively, and agree with Eq. (V28) of Ref. 26. The associated eigenfunctions are

$$\begin{aligned} \psi_\pm &= \sqrt{\frac{X \mp (\lambda-2)}{2X}}\,|^2\Pi_{1/2};\\ &1/2JM\rangle \mp \sqrt{\frac{X \pm (\lambda-2)}{2X}}\,|^2\Pi_{3/2};\\ &3/2JM\rangle. \end{aligned} \tag{A8}$$

In the notation of Sec. II,

$$c_1 = \sqrt{\frac{X \mp (\lambda-2)}{2X}}, \tag{A9}$$

and

$$c_2 = \sqrt{\frac{X \pm (\lambda-2)}{2X}}. \tag{A10}$$

Although these eigenvalues are widely available,[26] expressions for the corresponding eigenfunctions necessary in evaluating transition amplitudes are not.

APPENDIX B

Here we list the composite wave functions for $1\pi_g$ photoionization of O_2 ($^3\Sigma_g^-$) used to evaluate expressions in Eq. (14). The initial state wave functions are

$$M_s = 1{:}|1\pi_g^+ 1\pi_g^-|, \tag{B1a}$$

$$M_s = 0{:}\frac{1}{\sqrt{2}}\left[|1\pi_g^+ \bar{1}\pi_g^-| + |\bar{1}\pi_g^+ 1\pi_g^-|\right], \tag{B1b}$$

$$M_s = -1{:}|\bar{1}\pi_g^+ \bar{1}\pi_g^-|. \tag{B1c}$$

The final state wave functions for $\lambda = 0$, overall $^3\Pi_u$ symmetry are

$$M_s = 1{:}|1\pi_g^+ k\sigma_u|, \tag{B2a}$$

$$M_s = 0{:}\frac{1}{\sqrt{2}}\left[|1\pi_g^+ \bar{k}\sigma_u| + |\bar{1}\pi_g^+ k\sigma_u|\right], \tag{B2b}$$

$$M_s = -1{:}|\bar{1}\pi_g^+ \bar{k}\sigma_u|. \tag{B2c}$$

The final state wave functions for $\lambda = \pm 1$, overall $^3\Sigma_u^-$ symmetry are

$$M_s = 1{:}\frac{1}{\sqrt{2}}\left[|1\pi_g^+ k\pi_u^-| - |1\pi_g^- k\pi_u^+|\right], \tag{B3a}$$

$$\begin{aligned} M_s = 0{:}\frac{1}{2}&\left[|1\pi_g^+ \bar{k}\pi_u^-| - |\bar{\pi}_g^- k\pi_u^+| + |\bar{1}\pi_g^+ k\pi_u^-|\right. \\ &\left. - |1\pi_g^- \bar{k}\pi_u^+|\right], \end{aligned} \tag{B3b}$$

$$M_s = -1{:}\frac{1}{\sqrt{2}}\left[|\bar{1}\pi_g^+ \bar{k}\pi_u^-| - |\bar{1}\pi_g^- \bar{k}\pi_u^+|\right]. \tag{B3c}$$

The final state wave functions for $\lambda = -2$ of overall $^3\Pi_u$ symmetry are

$$M_s = 1{:}|1\pi_g^+ k\delta_u^-|, \tag{B4a}$$

$$M_s = 0{:}\frac{1}{\sqrt{2}}\left[|1\pi_g^+ \bar{k}\delta_u^-| + |\bar{1}\pi_g^+ k\delta_u^-|\right], \tag{B4b}$$

$$M_s = -1{:}|\bar{1}\pi_g^+ \bar{k}\delta_u^-|. \tag{B4c}$$

[1] X. Song, E. Sekreta, J. P. Reilly, H. Rudolph, and V. McKoy, J. Chem. Phys. **91**, 6062 (1989).
[2] H. Rudolph, J. A. Stephens, V. McKoy, and M. T. Lee, J. Chem. Phys. **91**, 1374 (1989).
[3] K. S. Viswanathan, E. Sekreta, E. R. Davidson, and J. P. Reilly, J. Chem. Phys. **90**, 5078 (1986).
[4] H. Rudolph, S. N. Dixit, V. McKoy, and W. M. Huo, Chem. Phys. Lett. **137**, 521 (1987).
[5] H. Rudolph, V. McKoy, and S. N. Dixit, J. Chem. Phys. **88**, 637 (1988).
[6] E. D. Poliakoff, J. C. K. Chan, and M. G. White, J. Chem. Phys. **85**, 6232 (1986).
[7] Ch. Jungen and D. Dill, J. Chem. Phys. **73**, 3338 (1980).
[8] D. Dill, Phys. Rev. A **6**, 160 (1972).
[9] K. Müller-Dethlefs, M. Sander, and E. W. Schlag, Chem. Phys. Lett. **112**, 291 (1984); M. Sander, L. A. Chewter, K. Müller-Dethlefs, and E. W. Schlag, Phys. Rev. A **36**, 4543 (1987).
[10] R. G. Tonkyn, J. W. Winniczek, and M. G. White, Chem. Phys. Lett. **164**, 137 (1989).
[11] R. G. Tonkyn, J. W. Winniczek, and M. G. White, J. Chem. Phys. **91**,

6632 (1989).
[12] K. S. Haber, Y. Jiang, G. Bryant, and E. R. Grant, and H. Lefebvre-Brion, Phys. Rev. A **44**, R5331 (1991).
[13] M. Braunstein, V. McKoy, S. N. Dixit, R. G. Tonkyn, and M. G. White, J. Chem. Phys. **93**, 5345 (1990).
[14] M. Braunstein and V. McKoy, J. Chem. Phys. **90**, 2575 (1989).
[15] T. Gustafsson, Chem. Phys. Lett. **75**, 505 (1980).
[16] P. M. Dittman, D. Dill, and J. L. Dehmer, J. Chem. Phys. **76**, 5703 (1982).
[17] G. Raseev, H. Lefebvre-Brion, H. Le Rouzo, and A. L. Roche, J. Chem. Phys. **74**, 6686 (1981).
[18] A. Gerwer, C. Asaro, B. V. McKoy, and P. W. Langhoff, J. Chem. Phys. **72**, 713 (1980).
[19] P. J. Miller, L. Li, W. A. Chupka, and S. D. Colson, J. Chem. Phys. **89**, 3921 (1988).
[20] J. A. Stephens, M. Braunstein, and V. McKoy, J. Chem. Phys. **89**, 3923 (1988).
[21] P. J. Miller, W. A. Chupka, J. Winniczek, and M. G. White, J. Chem. Phys. **89**, 4058 (1988).
[22] M. Braunstein, J. A. Stephens, and V. McKoy, J. Chem. Phys. **90**, 633 (1989).
[23] J. A. Stephens, M. Braunstein, and V. McKoy, J. Chem. Phys. **92**, 5319 (1990).
[24] P. J. Miller and W. A. Chupka (private communication).
[25] S. N. Dixit and V. McKoy, J. Chem. Phys. **82**, 3546 (1985).
[26] G. Herzberg, *Molecular Spectra and Molecular Structure: I. Spectra and Structure of Diatomic Molecules* (Krieger, Malabar, 1989).
[27] A. D. Buckingham, B. J. Orr, and J. M. Sichel, Philos. Trans. R. Soc. London, Ser. A **268**, 147 (1970).
[28] M. Mizushima, *The Theory of Rotating Diatomic Molecules* (Wiley–Interscience, New York, 1975).
[29] A. R. Edmonds, *Angular Momentum in Quantum Mechanics*, 2nd ed. (Princeton University, Princeton, 1974).
[30] J. T. Hougen, Natl. Bur. Stand. (U.S.) Monogr. 115 (1970).
[31] R. R. Lucchese, K. Takatsuka, and V. McKoy, Phys. Rep. **131**, 147 (1986).
[32] R. R. Lucchese, R. Raseev, and V. McKoy, Phys. Rev. A **25**, 2572 (1982).
[33] C. N. Yang, Phys. Rev. **74**, 764 (1948).
[34] See also, J. Xie and R. N. Zare, J. Chem. Phys. **93**, 3033 (1990).
[35] M. White and R. Tonkyn (private communication).
[36] See, for example, H. Rudolph, S. N. Dixit, V. McKoy, and W. M. Huo, J. Chem. Phys. **88**, 1516 (1988).
[37] D. G. McCoy, J. M. Morton, and G. V. Marr, J. Phys. B **11**, L547 (1978).
[38] T. A. Carlson, G. E. McGuire, A. E. Jonas, K. L. Cheng, C. P. Anderson, C. C. Lu, and B. P. Pullen, in *Electron Spectroscopy*, edited by D. A. Shirley (North–Holland, Amsterdam, 1972), pp. 207–31.
[39] W. H. Hancock and J. A. R. Samson, J. Electron Spectrosc. Relat. Phenom. **9**, 211 (1976).
[40] M. Nakamura and Y. Iida, in *Vacuum Ultraviolet Radiation Physics*, edited by E. E. Koch, R. Haensel, and C. Kunz, (Pergamon, Braunschweig, 1974), pp. 170–2.